JCI insight

Speed of lung inflation at birth influences the initiation of lung injury in preterm lambs

David G. Tingay, … , David W. Greening, Prue M. Pereira-Fantini

JCI Insight. 2024. https://doi.org/10.1172/jci.insight.181228.

Research In-Press Preview Inflammation Pulmonology

Gas flow is fundamental for driving tidal ventilation and thus the speed of lung motion, but current bias flow settings to support the preterm lung after birth are without an evidence base. We aimed to determine the role of gas bias flow rates to generate positive pressure ventilation in initiating early lung injury pathways in the preterm lamb. Using slower speeds to inflate the lung during tidal ventilation (gas flow rates 4-6 L/min) did not impact lung mechanics, mechanical power or gas exchange compared to those currently used in clinical practice (8-10 L/min). Speed of pressure and volume change during inflation were faster with higher flow rates. Lower flow rates resulted in less bronchoalveolar fluid protein, better lung morphology and fewer detached epithelial cells. Overall, relative to unventilated fetal controls, there was greater protein change using 8-10 L/min, which was associated with enrichment of acute inflammatory and innate responses. Slowing the speed of lung motion by supporting the preterm lung from birth with lower flow rates than currently used clinically resulted in less lung injury without compromising tidal ventilation or gas exchange.

Speed of lung inflation at birth influences the initiation of lung injury in preterm lambs

David G Tingay[1,2*], Monique Fatmous[1], Kelly Kenna[1], Jack Chapman[1,2], Ellen Douglas[1], Arun Sett[1,3,4], Qi Hui Poh[1], Sophia I Dahm[1], Tuyen Kim Quach[1,2], Magdy Sourial[1,5], Haoyun Fang[6,7], David W Greening[6,7,8], Prue M Pereira-Fantini[1,2]

[1]Neonatal Research, Murdoch Children's Research Institute, Parkville, Australia

[2]Department of Paediatrics, University of Melbourne, Melbourne, Australia

[3]Newborn Services, Joan Kirner Women's and Children's, Sunshine Hospital, Western Health, St Albans, Australia

[4]Department of Obstetrics and Gynaecology, University of Melbourne, Melbourne, Australia

[5]Translational Research Unit, Murdoch Children's Research Institute, Parkville, Australia

[6]Molecular Proteomics, Baker Heart and Diabetes Institute, Melbourne, Australia

[7]Baker Department of Cardiometabolic Health, The University of Melbourne, Melbourne, Australia

[8]Baker Department of Cardiovascular Research, Translation and Implementation, La Trobe University, Melbourne, Australia

Corresponding Author:

Prof David G Tingay MB BS DCH FRACP PhD

Neonatal Research

Murdoch Children's Research Institute

50 Flemington Rd.

Parkville 3052 Victoria

Australia

+61 3 9345 4023

david.tingay@mcri.edu.au

Running title: Gas flow and preterm lung injury

Manuscript word count: 7588 words

Conflicts of interest: DGT has presented at scientific meetings supported by Sentec AG and SLE UK Ltd. DGT has not received payment for presentations or consultation, and neither entity had input into content of presentations. The authors have no other competing interests to declare. PP-F holds provision patent (2023902862) filed with IP Australia related to protein biomarkers of preterm lung injury.

ABSTRACT

Gas flow is fundamental for driving tidal ventilation and thus the speed of lung motion, but current bias flow settings to support the preterm lung after birth do not have an evidence base. We aimed to determine the role of gas bias flow rates to generate positive pressure ventilation in initiating early lung injury pathways in the preterm lamb. Using slower speeds to inflate the lung during tidal ventilation (gas flow rates 4-6 L/min) did not impact lung mechanics, mechanical power or gas exchange compared to those currently used in clinical practice (8-10 L/min). Speed of pressure and volume change during inflation were faster with higher flow rates. Lower flow rates resulted in less bronchoalveolar fluid protein, better lung morphology and fewer detached epithelial cells. Overall, relative to unventilated fetal controls, there was greater protein change using 8-10 L/min, which was associated with enrichment of acute inflammatory and innate responses. Slowing the speed of lung motion by supporting the preterm lung from birth with lower flow rates than in current clinical use resulted in less lung injury without compromising tidal ventilation or gas exchange.

Word count: 182 words

Keywords: Resuscitation, Preterm infant, Lung injury, Gas flow, Rheotrauma

Abbreviations

$AaDO_2$	Alveolar Arterial Difference of Oxygen
ANOVA	Analysis of Variance
BALF	Bronchoalveolar Lavage Fluid
C_{dyn}	Dynamic respiratory system compliance
CI	Confidence Interval
DEC	Detached Epithelial Cell
DEP	Differentially Expressed Protein
EIT	Electrical Impedance Tomography
FDR	False Discovery Rate
GSEA	Gene set enrichment analysis
LLV	Left Lung Lavage
ME_{RS}	Mechanical Energy of the respiratory system
MP_{tidal}	Tidal Mechanical Power
NES	Normalised Enrichment Score
ΔP	Tidal change in pressure (Inflation pressure – PEEP)
$PaCO_2$	Arterial partial pressure of carbon dioxide
PaO_2	Arterial partial pressure of oxygen
PCA	Principal component analysis
PDGF	Platelet-derived growth factor
PEEP	Positive end-expiratory pressure
PPV	Positive Pressure Ventilation
RNA	Ribonucleic Acid
SpO_2	Peripheral oxygen saturation
Ti	Inspiratory Time
VEI	Ventilatory Efficacy Index

UVC	Unventilated Control
V_T	Tidal volume
VTV	Volume Targeted Ventilation
ΔV_L	Change in Lung Volume

INTRODUCTION

The lung is an organ that is in constant motion. Tidal ventilation involves the flow of gas during the mechanical process of inflation and deflation. Most preterm neonates need some form of positive pressure respiratory support after birth. Tidal volume (V_T) delivery requires a flow of gas to generate pressure and volume change. Despite delivered (or bias) gas flow rates being the fundamental mechanism supporting all positive pressure delivery systems, there are currently no guidelines for setting gas flow rates for neonates (1, 2). Ideally, the bias flow rate should facilitate effective tidal ventilation without imposing excessive work of breathing or injury.

Following birth, the structurally immature preterm lung is at high risk of lung injury (3-5). This is principally due to the mechanical stressors placed upon the lung during the motion of tidal ventilation (6, 7). Injury due to excessive tidal volume (volutrauma), driving pressure (ΔP; barotrauma) and/or inadequate positive end-expiratory pressure (PEEP; atelectasis-mediated injury) are well-documented (5, 8). The premise of injury from these mechanisms is based upon an absolute value causing injury. This is overly simplistic as each parameter occurs during continuous motion. The speed of pressure and volume change are likely to be just as important as the absolute amount of change on the fragile preterm lung; whether from direct shearing injury (rheotrauma) or excessive energy transfer (ergotrauma and mechanical power) (9).

The speed of pressure and volume change is determined by the relationship between airway gas flow and lung mechanics (especially resistance). Bias flow rates of 8-15 L/min are often used during neonatal resuscitation, and most modern neonatal ventilators have default flow rates between 8-10 L/min. In preterm lambs, flow rates of 8 L/min reduce lung injury compared to 18 and 28 L/min (10). There is a mechanical

and lung protective rationale for bias flow rates <8 L/min in the poorly compliant preterm lung with relatively normal airway resistance and short time constant. In a small study of preterm infants, flow rates of 4 L/min were able to support tidal ventilation (11). Mortality was lower compared to 8 L/min but the study was under-powered to reliably evaluate major outcomes. To our knowledge, no study has systematically evaluated the role of flow rates <8 L/min on preterm lung injury.

We hypothesise that the use of low gas flow rates to support positive pressure ventilation (PPV) support of the preterm lung will reduce early injury in the preterm lung. The primary aim of this study was to determine the role of gas flow rates on early lung injury in preterm lambs receiving lung protective PPV. The secondary aims included assessing the role of gas flow rates on **1)** effectiveness of ventilation, mechanical power, parameters of lung motion and regional ventilation and aeration, and **2)** the lung proteome composition.

RESULTS

Of the 89 lambs studied, Study 1 (15-min PPV+placental support) included 44 lambs and Study 2 (90-min PPV without placental support) 45 lambs. 3 and 4 lambs were excluded in Studies 1 and 2, respectively, due to fetal acidosis (pH<7.20; n=2), persistent metabolic acidosis during placental support PPV (n=2) or air leak (n=3). The included lambs were well-matched (Online Supplementary Table E1).

Characteristics of Tidal Lung Motion

Figure 1 summarises the changes in pressure (Figure 1A-C), volume (Figure 1D-F) and gas flow (Figure 1G-I) during tidal inflations (speed and acceleration of lung motion). The time to peak pressure and flow was slower with decreasing flow rates. Time to peak volume was a mean (95% CI) difference 94 (78,111) ms (t-test) slower between $F4_{90}$ and $F8_{90}$. There was no difference in the time to peak volume in the 15 min PPV groups (p=0.11; one-way ANOVA). The maximum rate of inflation pressure, volume and flow change (acceleration of volume) increased with increasing flow rates (all p<0.01). Time at maximum slope of the inflation pressure, volume and flow wave during inspiration shortened with increasing flow rates (all p<0.01; Online Supplementary Figure E1). There was no difference in maximum rate of expiratory pressure, volume and flow change (p=0.11-0.64).

Lung mechanics, aeration, ventilation and gas exchange

Figure 2 and 3 describe the lung mechanics for 15 and 90 min studies respectively. Maximum peak inspiratory flow approximated allocated target bias flows after completion of initial lung aeration at birth for the 15 min and 90 min study. There was no difference in dynamic respiratory system compliance (C_{dyn}), mechanical energy of the respiratory system (ME_{RS}), tidal change in pressure (ΔP), V_T, and tidal mechanical

power (MP_{tidal}) (Supplementary Figures E2 and E3) between all flow strategies during each study. ΔV_L from birth was similar during the 15 min study (Supplementary Figure E2C). Accurate ΔV_L from birth could not be calculated in the 90 min study due to artefact from birth handling at 3 min. Total lung capacity was a mean (95% CI) 4.2 (-2.1,10.5) mL/kg (one-way ANOVA) and 5.2 (-1.3,11.7) mL/kg (t-test) different in the $F4_{15}$ and $F4_{90}$ groups compared to respective F8 group (Figure 2D, 3D). In the 90 min study, the respiratory rate was lower in the $F4_{90}$ group (p=0.0026; mixed effects model; Figure 3E), although mean ventilatory efficiency index (VEI) was higher, the differences were not significant (p=0.53). There was no difference in pH, arterial partial pressure of carbon dioxide ($PaCO_2$), base excess, arterial partial pressure of oxygen (PaO_2), peripheral oxygen saturation (SpO_2), alveolar arterial difference in oxygen ($AaDO_2$) and carotid O_2 delivery (where applicable) (Online Supplementary Figure E4).

Lung aeration and ventilation homogeneity

Aeration was greater in the right (Figure 2E, 3F) and central lung regions, and relatively under-aerated in the most gravity dependent (dorsal) lung (Online Supplementary Figure E5) for all groups. The least gravity-dependent regions were preferentially aerated at 15 min (Study 1) but not 90 min (Study 2). Overall, aeration was more uniform, but not statistically different, during $F8_{15}$ and $F8_{90}$ than lower rates in all regions (all p=0.20-0.74). Regional ventilation was similar between all groups during each study, with heterogenous ventilation favouring the non-gravity dependent and right lung ventilation (Figure 2F and Online Supplementary Figure E6). Although $F4_{15}$ had fewer unventilated lung regions during Study 1, and following surfactant in Study 2 ($F4_{90}$), these differences were not statistically significant (Online Supplementary Figure E6; p=0.10 and 0.33).

Haemodynamics

There was no difference in heart rate or carotid artery blood flow between any flow strategies (Online Supplementary Figure E7).

Lung morphology and injury

Protein concentration of left lung bronchoalveolar lavage fluid (BALF) increased with increasing flow rates at both 15 and 90 min (p=0.0003 and 0.047 respectively; one-way ANOVA), with no difference between an unventilated fetal control group (UVC) and 4 L/min groups (Figure 4). Histological indicators of lung morphology and injury are shown in Figure 5 and Online Supplementary Figure E8. Overall, the $F4_{90}$ group resulted in fewer alveoli per field of view, the most airspace and fewer detached epithelial cells at 90 min.

Proteome analysis

1543 proteins from Study 1 and 2588 proteins from Study 2 were included in proteome analysis (Online Supplementary Tables E2-5). In principal component analysis (PCA), a high degree of separation was apparent between the UVC group and all flow groups in the non-gravity dependent lung at 15 min (Figure 6A), while moderate separation was observed in the gravity-dependent lung (Figure 6B). There was no separation between UVC and flow group proteomes in either lung region at 90 min (Figure 6C-D).

Differentially expressed proteins (DEPs) were identified in all ventilation groups (Figure 6E-R, Online Supplementary Table 6), except the $F6_{15}$ gravity-dependent lung, with non-gravity dependent lung regions containing more DEPs compared to gravity-dependent lung. DEPs commonly identified between $F4_{15}$, $F6_{15}$ and $F8_{15}$ displayed

similar protein abundance (relative to UVC), whereas DEPs at 90 min displayed a greater magnitude of change in $F8_{90}$ compared to $F4_{90}$ (Figure 6S-T). Nine of the top 10 proteins that increased in abundance in $F8_{90}$ compared to $F4_{90}$ were associated with the innate immune response and acute inflammatory response, specifically neutrophil degranulation (Figure 6U). When comparing DEPs between Studies 1 and 2, common proteins were only identified in non-gravity dependent lung proteomes, with RPS3A, RPL10, and CORO1A co-identified between $F4_{15}$ and $F4_{90}$ groups, and CAST, TMA7, NUMA1 and LCP1 co-identified between $F8_{15}$ and $F8_{90}$ groups.

To gain an understanding of protein function and classification, DEPs were analysed using the PANTHER database. In the non-gravity dependent lung, 83% (Study 1) and 71% (Study 2) of biological processes were commonly identified in all flow groups (Online Supplementary Figure E9A). The diversity of these processes was comparable in the $F8_{15}$ gravity-dependent lung but reduced in the $F4_{15}$ gravity-dependent lung. This was mirrored in further analysis of cellular processes and protein class characterisation (Online Supplementary Figure E9B-C). At 90 min, differences between $F4_{90}$ and $F8_{90}$ non-gravity dependent and gravity-dependent lung were more obvious.

Gene set enrichment analysis (GSEA) using the Reactome database identified 19 enriched and 22 depleted biological pathways in the non-gravity dependent lung, and 11 enriched and 19 depleted biological pathways in the gravity-dependent lung that were statistically significant (FDR<0.05; Figure 7). 8-10 L/min flow had the greatest impact across time and lung regions. In the non-gravity dependent lung, hemostasis and signal transduction pathways were enriched in the flow groups at 15 min, and decreased developmental biology pathways at 90 min, which was less apparent in the gravity-dependent lung. At 90 min only, $F4_{90}$ was associated with increased platelet-derived

growth factor (PDGF) signalling, which was not seen in the F8 group. Metabolism of RNA was most consistently depleted in flow groups and lung regions.

DISCUSSION

Preterm birth requires the lung to transition from a fluid-filled to aerated state, and then maintain ongoing tidal ventilation despite surfactant-deficiency and structural immaturity (7). Initial lung aeration and subsequent recruitment is actively driven by tidal inflations (4, 12). The neonatal lung does not aerate uniformly and, in preclinical studies, this state of volume heterogeneity is strongly associated with injury (4, 12). Our study aimed to explore the role of tidal lung motion on lung injury, specifically the shear stresses (rheotrauma) caused by the speed of pressure and volume change driven by bias gas flow. We found in our lamb population that supporting the preterm lung with bias flow rates of 4-6 L/min reduced lung injury compared to 8-10 L/min. Most neonatal ventilators, and T-Piece resuscitation devices being used in the delivery room, deliver or have recommendation to set bias flows at 8-10 L/min (1, 2). To the best of our knowledge, this is the first time that currently used bias flow rates have been shown to be injurious.

The role of tissue motion in preterm lung injury has been inadequately studied, limited to a single lamb study and small clinical human study (10, 11). In contrast, vascular shear stress and resultant injury is well described (13, 14). There is a strong rationale for flow-related lung injury in the preterm lung. The preterm respiratory system has a low resistance and compliance. This scenario places few brakes on rapid lung motion once enough inflation pressure is applied during both spontaneous breathing and PPV (3). Furthermore, the preterm lung is not yet adapted to the movement of air, or the flow rates required to support gas exchange. Preterm lung injury is generally defined by the impact of the absolute magnitude of a parameter, such as V_T, inflating pressures, positive end-expiratory pressure (PEEP) and lung volume (V_L) (5, 6). In our study, we applied a standardised ventilation strategy that conformed with the current concepts to

minimise injury from these mechanisms in preterm lambs; avoidance of excessive V_T, inflating pressure and atelectasis (dynamic PEEP at birth followed by 8 cmH_2O PEEP), antenatal steroid exposure and surfactant treatment (Study 2) (3, 4, 15-17). Bias flow was the only ventilator-derived parameter that differed between groups, suggesting the increase in total protein concentration and different alveolar morphology observed at 15 and 90 min was due to the independent impact of the higher flow rates.

As the duration of PPV increased, the $F8_{90}$ group demonstrated increased alteration in the immune response and acute inflammatory proteome compared to $F4_{90}$. This likely reflects an acute injurious impact from the higher flow rates, as demonstrated by the increase in detached epithelial cells. This mechanotransducive injury from flow is likely multifactorial, including tissue shear stress, acceleration, different flow types, energy transference and direct pressure and volume impact. Our study could not delineate the mechanism of injury, but the different processes and protein classes seen throughout lung regions, and similar ME_{RS} values, suggests that considering rheotrauma as simply shear stress or force-related energy transfer may be too simplistic. Interestingly, $F4_{90}$ was associated with increased PDGF signalling important for alveolarisation, with defective signalling being a primary feature of bronchopulmonary dysplasia in humans (18, 19). It is possible that the slower flow rates allow alveolar cells to adapt better to the increased mechanical tensions associated with ventilation after birth (20).

There was greater differentiation in the proteome for all flow rates against UVC in the non-gravity dependent lung. This is to be expected as aeration and ventilation patterns favoured the non-dependent regions. The differences in protein classes, processes and pathways between gravity-dependent lung regions further illustrates the need to define preterm lung injury based on regional heterogeneity. Unfortunately, the differences in

right and left injury patterns could not be assessed. Although there were differences in lung morphology between UVC and flow groups, the findings were more subtle than other studies with smaller sample sizes, (21-23) and likely reflects the more lung protective approach to ventilation in our study.

Lower bias flow rates did not negatively impact lung mechanics or gas exchange. This is important and supports the need for clinical investigation of lower bias flow rates, and importantly slower rates of pressure and volume changes during invasive support. A previous study from 1968 of different gas flow rates in 9 neonates supported using a slow rate and long Ti approach for oxygenation, but this approach is now considered injurious (6, 24). The similar VEI between the $F4_{90}$ and $F8_{90}$ groups was achieved due to the lower respiratory rate in the $F4_{90}$ group, suggesting a similar response to that reported by Bach and colleagues in term lambs (25). Importantly, respiratory rate was titrated to maintain the $PaCO_2$ target and Ti fixed. This indicates that CO_2 clearance was improved in the $F4_{90}$ group likely related to less lung injury. We did not measure the impact of flow rates on ventilation-perfusion matching. This maybe impacted by the lower mean airway pressure resulting from the longer pressure rise time during inflation at slower flow rates and should be considered in future studies.

Many modern ventilators do not allow direct titration of bias flow. Rather the clinician can alter the pressure rise time. In experienced hands, arguably this is a more clinically usable approach. Physiologically, the Ti should first be set to the time constant of the lung (compliance × resistance) and titrated to the flow wave shape (26). Thereafter, our data suggests that the rise time can be slowed to obtain end-inspiratory pressure near the end of Ti. Such an approach will account for the variability in optimal flow rates due to difference in lung maturation (gestation) and mechanics (disease severity) (24).

Whether lower flow rates can be tolerated during non-invasive ventilation cannot be concluded from this study. We did not measure work of breathing in our study, and increased work of breathing may generate rapid inspiratory flows. Studies in neonates of bias flow during non-invasive ventilation need to include measures of work of breathing (such as oesophageal manometry). Given the simplicity of altering bias flow during non-invasive support, and the lack of guidance for clinicians, (1, 2) there is a clear need to understand its role in preterm injury.

In our study, we used a continuous bias flow ventilator, a mechanism of pressure delivery similar to T-piece devices used in the delivery room. Peak inspiratory flow rates approximated but were not always equal to the set bias flow. This is not surprising, although bias flow and inspiratory flow are nearly linear, (25) pressure gradient drops through the circuit and endotracheal tube, laminar and turbulent flow patterns through the airway, changing respiratory mechanics and the mechanism of titrating bias flow in the SLE5000 will all alter flow rates (27). This is especially so during the birth transition when all these factors are likely to be greater as the lung transitions from a high-resistance fluid to low-resistance aerated state (4, 12, 28).

There are additional limitations to our study, some of which we have reported in detail before, including those related to EIT and proteomics (3, 4, 29-31). There were more female lambs in Study 2 relative to male lambs, and the opposite in Study 1. This may have influenced the injury outcomes and could, in part, explain the higher protein concentrations in Study 1 despite the shorter ventilation period. Although the lambs in Study 1 were also more immature and did not receive surfactant. The study was not powered to sub-group analysis by sex. Unlike human neonates, the lambs were apnoeic and intubated. This approach, though well established, (32) limits translation to the

clinical setting and was intentional. Spontaneous breathing generates negative flow inspiratory gradients, which in themselves may generate injury, especially in the delivery room where spontaneous inflations may not be synchronous with PPV-mediated inflations. This would create very complex flow patterns involving variable turbulent and laminar flow states. Our aim was to understand both the initiation and potentiation of early lung injury, necessitating the established but non-clinical prolonged placental support model in Study 1 (21). Allowing spontaneous breathing during placental support whilst maintaining ewe and fetal analgesia is technically and ethically difficult. This justifies why we chose different gestational age ranges. Study 1 was embedded in a larger program in 124-127d gestation lambs also differentiating the roles of inflating pressure and V_T on initiating lung injury, (3, 33) but are at a gestation that is harder to achieve spontaneous breathing at birth (34). We also wanted to understand the independence of flow-mediated lung injury. Now the role of PPV is better understood, these can be interrogated during different permutations of non-invasive and invasive support with synchronous and asynchronous breathing in the future.

Conclusions

Set bias flow and resultant speed of pressure and volume change in the lung during tidal ventilation are independent mechanisms of neonatal lung injury that have been largely under-recognised. This study demonstrates that supporting the preterm lung from birth with slower flow rates than currently used clinically may result in less lung injury without compromising tidal ventilation or gas exchange. If replicated in human studies, implementing lower gas flow rates into neonatal care maybe a simple and cost-effective method of lung protection.

METHODS

Sex as a biological variable

For this study, both male and female preterm Border-Leicester cross lambs were studied. Randomisation to allocated flow strategy occurred before birth and sex was not known at randomisation. Similar findings are reported for both sexes. Sex may have been a variable but power to sex as a variable was not possible for reasons of ethically reduction.

A detailed methodology is available in the online supplement. Some aspects of the methodology have been reported previously (3, 4, 35, 36). To address the study aims, two consecutive studies were performed (Figure 8). The first aimed to determine the role of bias flow rates on initiating early lung injury pathways at birth (**Study 1**). For Study 1, 124-127d preterm Border-Leicester cross lambs (term~145d) were studied during 15 min of positive pressure ventilation (PPV) whilst on placental support using 4 ($F4_{15}$), 6 ($F6_{15}$) and 8-10 ($F8_{15}$) L/min flow (n=10-11/group). Lambs were then maintained apnoeic on placental support for 30 min to allow expression of injury markers (3, 21, 33).

Study 2 investigated the role of 4-6 ($F4_{90}$) versus 8-10 ($F8_{90}$) L/min flow (n=15-17/group) on potentiation of lung injury during 90 min of PPV without placental support in 126-129d lambs. The flow rates and group sizes for Study 2 were informed by the results of Study 1 to ensure likelihood of treatment difference and maximise animal reduction. Group allocation was randomly applied in both studies. 11-13 lambs per study were also studied as unventilated controls (UVC) for injury comparisons.

Experimental Instrumentation

All lambs were born via caesarean section to glucocorticoid treated ewes and intubated and instrumented as described previously (3, 37). Following full exteriorisation, all lambs were ventilated supine with active warming. Anaesthesia and analgesia were maintained with ketamine and midazolam infusions.

Measurements

Heart rate, carotid artery pressure and flow, airway pressure, gas flow and V_T at the airway opening (Florian, Acutronic Medical Systems, Hirzel, Switzerland) were measured continuously from birth. Global and regional lung volume changes were acquired by electrical impedance tomography (EIT; Pioneer System, Sentec, Landquart, Switzerland) at 48 scans/s (37). Arterial blood analysis was performed at 5 min and then every 15 min from ventilation onset.

Ventilation Strategies and general management after birth

Except for allocated bias flow, a common PPV strategy (SLE5000, SLE Ltd, South Croydon, UK) was employed in accordance with current lung protective concepts summarised in Figure 1. Lambs in Study 2 received the initial 3 min of PPV with placental support to mimic deferred cord clamping. Inspiratory time (Ti) was commenced at 0.5s and shortened if end-inspiratory 0 L/min flow was >20% of Ti. Lambs in Study 2 received 240 mg of porcine surfactant (Curosurf, Chiesi, Parma, Italy) at 10 min. At the end of assigned experimental period, a bronchoalveolar lavage was performed and the static *in vivo* pressure-volume (PV) curve generated from atmosphere to 35 cmH_2O to determine static lung mechanics (3, 4). Then a lethal dose of pentobarbitone was administered (35-39).

Data Acquisition and Analysis

EIT data, inflating pressure (ΔP), V_T, dynamic respiratory system compliance (C_{dyn}) and minimum (diastolic), maximum (systolic) and average carotid blood flow were calculated at key time points (3, 4, 16, 40). Dynamic tidal mechanical power (MP_{tidal}) (41), mechanical energy of the respiratory system (ME_{RS})(42) and ventilatory efficacy index (VEI) were calculated post-hoc (see online supplementary methods for formulas) (23, 25, 43). Time-course EIT image data were reconstructed using an anatomically correct custom-built lamb algorithm (31, 36, 44) filtered to the respiratory domain (IBEX software package, Sentec) (37). Change in lung volume (ΔV_L) from the pre-aerated state was calibrated from the static pressure-volume (PV) curve (35, 39). Relative aeration (to anatomical size) (36, 37, 39) and centre of ventilation (CoV) within the gravity dependent and non-dependent regions, and right and left lungs were calculated (31).

Protein concentration of left lung bronchoalveolar lavage fluid (BALF) were determined using the Lowry method (45). Histology of the dependent and non-dependent zones of the right upper lobe (fixed at 20 cmH_2O) were assessed using our previously described standardised criteria in ImageJ as detailed in the supplementary methods (29, 36, 39, 46).

Lung tissue samples were collected from the gravity dependent and non-dependent zones of the right lower lobe for quantitative mass spectrometry-based proteomics using our previously detailed methods (3, 33). Comparisons between ventilated groups *versus* study-specific UVC groups were performed using the EdgeR Package (RStudio) to identify differentially expressed proteins (DEPs), with significance set to false discover rate (FDR) <0.05 (47, 48). Gene set enrichment analysis (GSEA) was

performed in Webgestalt to identify altered biological pathways within the Reactome database, with FDR<0.05, (49) and PANTHER was used to characterise biological processes and protein classes of DEPs (50).

Statistical Analysis

8-10 lambs/group were previously able to demonstrate differences in our histological markers following 15 min of PPV, (3, 51) and 15-20/gp following 90 min PPV at each allocated gestation (80% type 1 error, p=0.05) (4). All non-proteomics data were investigated with either t-tests, one-way ANOVA or mixed effects analysis (ventilation strategy and time as variables) and appropriate post-test analysis. A p value less than 0.05 was considered significant.

Study Approval

All techniques and procedures were approved by the Animal Ethics Committee of the Murdoch Children's Research Institute, Melbourne, Australia (4 May 2020; A923, 23 September 2021; A943, 3 August 2022; A956) in accordance with National Health and Medical Research Council guidelines (Australia). The ARRIVE Statement for this study is available at Tingay, David (2022): University of Melbourne https://doi.org/10.26188/25242616.v1

Data availability

All data, including raw data used for all figures and analysis, and allocation of specific subjects in previously published material is available upon request to the corresponding author from three months following article publication to researchers who provide a methodologically sound proposal, with approval by an independent review committee ("learned intermediary"). Proposals should be directed to david.tingay@mcri.edu.au to

gain access. Data requestors will need to sign a data access or material transfer agreement approved by MCRI. The ARRIVE Statement for this study and all the proteome datasets used for analysis are available at Tingay, David (2024): University of Melbourne. https://doi.org/10.26188/25242616.v1 and https://doi.org/10.26188/25242589. The mass spectrometry proteomics data have been deposited to the ProteomeXchange Consortium (http://proteomecentral.proteomexchange.org) via the PRIDE partner repository with the dataset identifier PXD041917 (Study 1) and PXD050305 (Study 2). Value for all data points in graphs are reported in the Supporting Data Values file.

Author contributions: DGT and PP-F developed the concept, designed the experiment and interpreted the data. DGT, PP-F, JC, KK, ED, AS, SID, MS, MF were involved in lamb experimental work. QHP, DWG, HF, MF, PP-F performed proteomic experiments and MF, TKQ and PP-F performed the injury and proteomics analysis. DGT supervised all aspects of the study and subsequent data analysis. JC, KK, SID, ED and DGT performed the ventilator waveform signal and EIT analysis. All authors participated in data interpretation under supervision of DGT and PP-F. DGT wrote the first draft and all authors contributed to redrafting the manuscript.

Acknowledgments: The authors acknowledge Rebecca Sutton for assistance in preparation of the ewes. The Proteomics & Metabolomics Platform at La Trobe University, and Shuai Nie and Nick Williamson from Melbourne Mass Spectrometry and Proteomics Facility at the Bio21 Molecular Science and Biotechnology Institute, University of Melbourne, for providing facility access, supporting proteomic experimental design, and running proteomic samples on their mass spectrometers. Avinash Kondiboyina for generating a macro script to input in FIJI for histological analysis of the lung. Andreas Waldmann (previously at Sentec AG) for assisting in EIT analysis scripts. Dr Kristin Ferguson and Jean Hellstern for comments and suggestions on the manuscript. DGT wishes to acknowledge Dr K Bach (Auckland, New Zealand) and Prof JJ Pillow (University of Western Australia) for originally suggesting the need to better understand flow-related injury in the preterm lung.

Financial Support: This study is supported by a National Health and Medical Research Council Ideas Grant (Grant ID 1182676) and the Victorian Government Operational Infrastructure Support Program (Melbourne, Australia). DGT is supported by a

National Health and Medical Research Council Clinical Career Development Fellowship (Grant ID 1123859) and Leadership Level 1 Investigator Grant (Grant ID 2008212). Sentec AG (Landquart, Switzerland) manufactured EIT belts custom-built for lambs for this study. All EIT hardware was purchased by Murdoch Children's Research Institute. Sentec AG were not involved in study design, implementation, analysis, interpretation or reporting.

REFERENCES

1. Sweet DG, Carnielli VP, Greisen G, Hallman M, Klebermass-Schrehof K, Ozek E, et al. European Consensus Guidelines on the Management of Respiratory Distress Syndrome: 2022 Update. *Neonatology.* 2023;120(1):3-23.
2. Madar J, Roehr CC, Ainsworth S, Ersdal H, Morley C, Rudiger M, et al. European Resuscitation Council Guidelines 2021: Newborn resuscitation and support of transition of infants at birth. *Resuscitation.* 2021;161:291-326.
3. Tingay DG, Fatmous M, Kenna K, Dowse G, Douglas E, Sett A, et al. Inflating Pressure and Not Expiratory Pressure Initiates Lung Injury at Birth in Preterm Lambs. *Am J Respir Crit Care Med.* 2023;208(5):589-99.
4. Tingay DG, Pereira-Fantini PM, Oakley R, McCall KE, Perkins EJ, Miedema M, et al. Gradual Aeration at Birth Is More Lung Protective Than a Sustained Inflation in Preterm Lambs. *Am J Respir Crit Care Med.* 2019;200(5):608-16.
5. Bjorklund LJ, Ingimarsson J, Curstedt T, John J, Robertson B, Werner O, et al. Manual ventilation with a few large breaths at birth compromises the therapeutic effect of subsequent surfactant replacement in immature lambs. *Pediatr Res.* 1997;42(3):348-55.
6. Thebaud B, Goss KN, Laughon M, Whitsett JA, Abman SH, Steinhorn RH, et al. Bronchopulmonary dysplasia. *Nat Rev Dis Primers.* 2019;5(1):78.
7. Jobe AH, Hillman N, Polglase G, Kramer BW, Kallapur S, and Pillow J. Injury and inflammation from resuscitation of the preterm infant. *Neonatology.* 2008;94(3):190-6.
8. Dreyfuss D, and Saumon G. Ventilator-induced lung injury: lessons from experimental studies. *Am J Respir Crit Care Med.* 1998;157(1):294-323.

9. Kneyber MCJ. Driving Pressure and Mechanical Power: The Return of Physiology in Pediatric Mechanical Ventilation. *Pediatr Crit Care Med.* 2021;22(10):927-9.
10. Bach KP, Kuschel CA, Hooper SB, Bertram J, McKnight S, Peachey SE, et al. High bias gas flows increase lung injury in the ventilated preterm lamb. *PLoS One.* 2012;7(10):e47044.
11. Bach KP, Kuschel CA, Patterson N, Skwish H, Huth S, Phua HH, et al. Effect of Bias Gas Flow on Tracheal Cytokine Concentrations in Ventilated Extremely Preterm Infants: A Randomized Controlled Trial. *Neonatology.* 2021;118(3):332-9.
12. Tingay DG, Farrell O, Thomson J, Perkins EJ, Pereira-Fantini PM, Waldmann AD, et al. Imaging the Respiratory Transition at Birth: Unravelling the Complexities of the First Breaths of Life. *Am J Respir Crit Care Med.* 2021;204(1):82-91.
13. Cameron JN, Mehta OH, Michail M, Chan J, Nicholls SJ, Bennett MR, et al. Exploring the relationship between biomechanical stresses and coronary atherosclerosis. *Atherosclerosis.* 2020;302:43-51.
14. Mynard JP, Kondiboyina A, Kowalski R, Cheung MMH, and Smolich JJ. Measurement, Analysis and Interpretation of Pressure/Flow Waves in Blood Vessels. *Front Physiol.* 2020;11:1085.
15. Tingay DG, Togo A, Pereira-Fantini PM, Miedema M, McCall KE, Perkins EJ, et al. Aeration strategy at birth influences the physiological response to surfactant in preterm lambs. *Arch Dis Child Fetal Neonatal Ed.* 2019;104(6):F587-F93.

16. Tingay DG, Bhatia R, Schmolzer GM, Wallace MJ, Zahra VA, and Davis PG. Effect of sustained inflation vs. stepwise PEEP strategy at birth on gas exchange and lung mechanics in preterm lambs. *Pediatr Res.* 2014;75(2):288-94.
17. Klingenberg C, Wheeler KI, McCallion N, Morley CJ, and Davis PG. Volume-targeted versus pressure-limited ventilation in neonates. *Cochrane Database Syst Rev.* 2017;10:CD003666.
18. Fulton CT, Cui TX, Goldsmith AM, Bermick J, and Popova AP. Gene Expression Signatures Point to a Male Sex-Specific Lung Mesenchymal Cell PDGF Receptor Signaling Defect in Infants Developing Bronchopulmonary Dysplasia. *Sci Rep.* 2018;8(1):17070.
19. Popova AP, Bentley JK, Cui TX, Richardson MN, Linn MJ, Lei J, et al. Reduced platelet-derived growth factor receptor expression is a primary feature of human bronchopulmonary dysplasia. *Am J Physiol Lung Cell Mol Physiol.* 2014;307(3):L231-9.
20. Cavanaugh KJ, Jr., Oswari J, and Margulies SS. Role of stretch on tight junction structure in alveolar epithelial cells. *Am J Respir Cell Mol Biol.* 2001;25(5):584-91.
21. Hillman NH, Kemp MW, Noble PB, Kallapur SG, and Jobe AH. Sustained inflation at birth did not protect preterm fetal sheep from lung injury. *Am J Physiol Lung Cell Mol Physiol.* 2013;305(6):L446-53.
22. Tingay DG, Wallace MJ, Bhatia R, Schmolzer GM, Zahra VA, Dolan MJ, et al. Surfactant before the first inflation at birth improves spatial distribution of ventilation and reduces lung injury in preterm lambs. *J Appl Physiol.* 2014;116(3):251-8.

23. Ikegami M, Jobe AH, Newnham J, Polk DH, Willet KE, and Sly P. Repetitive prenatal glucocorticoids improve lung function and decrease growth in preterm lambs. *Am J Respir Crit Care Med.* 1997;156(1):178-84.
24. Owen-Thomas JB, Ulan OA, and Swyer PR. The effect of varying inspiratory gas flow rate on arterial oxygenation during IPPV in the respiratory distress syndrome. *Br J Anaesth.* 1968;40(7):493-502.
25. Bach KP, Kuschel CA, Oliver MH, and Bloomfield FH. Ventilator gas flow rates affect inspiratory time and ventilator efficiency index in term lambs. *Neonatology.* 2009;96(4):259-64.
26. Salazar E, and Knowles JH. An Analysis of Pressure-Volume Characteristics of the Lungs. *J Appl Physiol.* 1964;19:97-104.
27. Jarreau PH, Louis B, Dassieu G, Desfrere L, Blanchard PW, Moriette G, et al. Estimation of inspiratory pressure drop in neonatal and pediatric endotracheal tubes. *J Appl Physiol.* 1999;87(1):36-46.
28. Gaertner VD, Buchler VL, Waldmann A, Bassler D, and Ruegger CM. Deciphering Mechanisms of Respiratory Foetal-to-Neonatal Transition in Very Preterm Infants. *Am J Respir Crit Care Med.* 2023.
29. Oakley RB, Tingay DG, McCall KE, Perkins EJ, Sourial M, Dargaville PA, et al. Gestational Age Influences the Early Microarchitectural Changes in Response to Mechanical Ventilation in the Preterm Lamb Lung. *Front Pediatr.* 2019;7:325.
30. Pereira-Fantini PM, Byars SG, McCall KE, Perkins EJ, Oakley RB, Dellaca RL, et al. Plasma proteomics reveals gestational age-specific responses to mechanical ventilation and identifies the mechanistic pathways that initiate preterm lung injury. *Sci Rep.* 2018;8(1):12616.

31. Frerichs I, Amato MB, van Kaam AH, Tingay DG, Zhao Z, Grychtol B, et al. Chest electrical impedance tomography examination, data analysis, terminology, clinical use and recommendations: consensus statement of the TRanslational EIT developmeNt stuDy group. *Thorax.* 2017;72(1):83-93.
32. Lambert CJ, Hooper SB, Te Pas AB, and McGillick EV. Improving Newborn Respiratory Outcomes With a Sustained Inflation: A Systematic Narrative Review of Factors Regulating Outcome in Animal and Clinical Studies. *Front Pediatr.* 2020;8:516698.
33. Pereira-Fantini PM, Kenna KR, Fatmous M, Sett A, Douglas E, Dahm S, et al. Impact of tidal volume strategy at birth on initiating lung injury in preterm lambs. *Am J Physiol Lung Cell Mol Physiol.* 2023;325(5):L594-L603.
34. Milesi I, Tingay DG, Lavizzari A, Bianco F, Zannin E, Tagliabue P, et al. Supraglottic Atomization of Surfactant in Spontaneously Breathing Lambs Receiving Continuous Positive Airway Pressure. *Pediatr Crit Care Med.* 2017;18(9):e428-e34.
35. Tingay DG, Rajapaksa A, Zannin E, Pereira-Fantini PM, Dellaca RL, Perkins EJ, et al. Effectiveness of individualized lung recruitment strategies at birth: an experimental study in preterm lambs. *Am J Physiol Lung Cell Mol Physiol.* 2017;312(1):L32-L41.
36. Tingay DG, Rajapaksa A, Zonneveld CE, Black D, Perkins EJ, Adler A, et al. Spatiotemporal Aeration and Lung Injury Patterns Are Influenced by the First Inflation Strategy at Birth. *Am J Respir Cell Mol Biol.* 2016;54(2):263-72.
37. McCall KE, Waldmann AD, Pereira-Fantini P, Oakley R, Miedema M, Perkins EJ, et al. Time to lung aeration during a sustained inflation at birth is influenced by gestation in lambs. *Pediatr Res.* 2017;82(4):712-20.

38. Tingay DG, Polglase GR, Bhatia R, Berry CA, Kopotic RJ, Kopotic CP, et al. Pressure-limited sustained inflation vs. gradual tidal inflations for resuscitation in preterm lambs. *J Appl Physiol.* 2015;118(7):890-7.
39. Tingay DG, Lavizzari A, Zonneveld CE, Rajapaksa A, Zannin E, Perkins E, et al. An individualized approach to sustained inflation duration at birth improves outcomes in newborn preterm lambs. *Am J Physiol Lung Cell Mol Physiol.* 2015;309(10):L1138-49.
40. Dahm SI, Kenna KR, Stewart D, Pereira-Fantini PM, McCall KE, Perkins EJ, et al. Aeration strategy at birth does not impact carotid haemodynamics in preterm lambs. *Pediatr Res.* 2023;93(5):1226-32.
41. Becher T, van der Staay M, Schadler D, Frerichs I, and Weiler N. Calculation of mechanical power for pressure-controlled ventilation. *Intensive Care Med.* 2019;45(9):1321-3.
42. Kneyber MCJ, Ilia S, Koopman AA, van Schelven P, van Dijk J, Burgerhof JGM, et al. Energy transmission in mechanically ventilated children: a translational study. *Crit Care.* 2020;24(1):601.
43. Notter RH, Egan EA, Kwong MS, Holm BA, and Shapiro DL. Lung surfactant replacement in premature lambs with extracted lipids from bovine lung lavage: effects of dose, dispersion technique, and gestational age. *Pediatr Res.* 1985;19(6):569-77.
44. Adler A, Arnold JH, Bayford R, Borsic A, Brown B, Dixon P, et al. GREIT: a unified approach to 2D linear EIT reconstruction of lung images. *Physiol Meas.* 2009;30(6):S35-55.
45. Lowry OH, Rosebrough NJ, Farr AL, and Randall RJ. Protein measurement with the Folin phenol reagent. *J Biol Chem.* 1951;193(1):265-75.

46. Schneider CA, Rasband WS, and Eliceiri KW. NIH Image to ImageJ: 25 years of image analysis. *Nat Meth.* 2012;9(7):671-5.
47. Lun AT, Chen Y, and Smyth GK. It's DE-licious: A Recipe for Differential Expression Analyses of RNA-seq Experiments Using Quasi-Likelihood Methods in edgeR. *Methods Mol Biol.* 2016;1418:391-416.
48. Robinson MD, McCarthy DJ, and Smyth GK. edgeR: a Bioconductor package for differential expression analysis of digital gene expression data. *Bioinformatics.* 2010;26(1):139-40.
49. Liao Y, Wang J, Jaehnig EJ, Shi Z, and Zhang B. WebGestalt 2019: gene set analysis toolkit with revamped UIs and APIs. *Nucleic Acids Res.* 2019;47(W1):W199-W205.
50. Thomas PD, Ebert D, Muruganujan A, Mushayahama T, Albou LP, and Mi H. PANTHER: Making genome-scale phylogenetics accessible to all. *Protein Sci.* 2022;31(1):8-22.
51. Pereira-Fantini PM, Pang B, Byars SG, Oakley RB, Perkins EJ, Dargaville PA, et al. Preterm Lung Exhibits Distinct Spatiotemporal Proteome Expression at Initiation of Lung Injury. *Am J Respir Cell Mol Biol.* 2019;61(5):631-42.

FIGURE LEGENDS

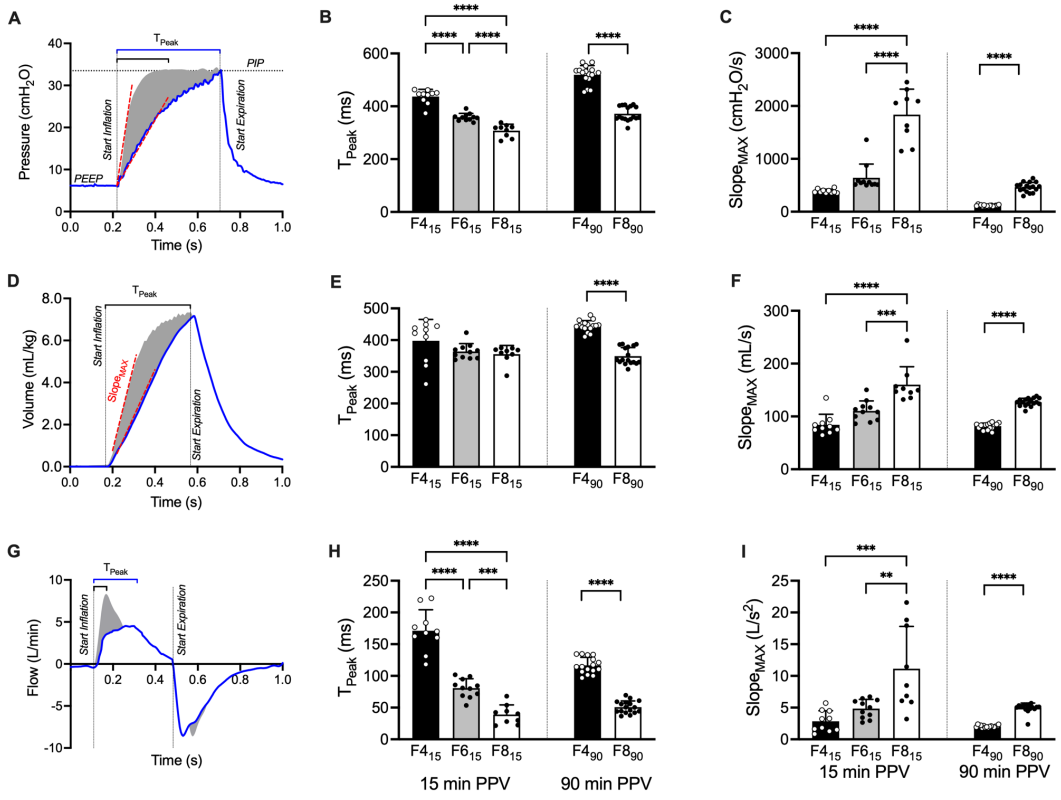

Figure 1. Characteristics of tidal lung motion. Representative pressure (**A**), tidal volume (**D**) and flow (**G**) wave during a single respiratory cycle at 4 L/min (blue line) and 8 L/min wave (grey shaded area). Time to inspiratory peak (T_{Peak}) for pressure (**B**), volume (**E**) and flow (**H**) wave. Maximum slope of the inspiratory ($Slope_{MAX}$) pressure (**C**), volume (**F**) and flow (**I**) wave. $Slope_{MAX}$ represents the maximum speed of pressure and volume change, and $Slope_{MAX}$ of flow the acceleration of volume in the lung. Black bars represent 4 L/min ($F4_{15}$ and $F4_{90}$) groups, grey bars 6 L/min ($F6_{15}$) and white 8-10 L/min ($F8_{15}$ and $F8_{90}$) bias flow strategy for each ventilation period. Dots represent individual lambs, bars mean and error bars SD. * $p<0.05$, ** $p<0.01$, *** $p<0.001$, **** $p<0.0001$ Tukey post-test (mixed effects model) or t-test.

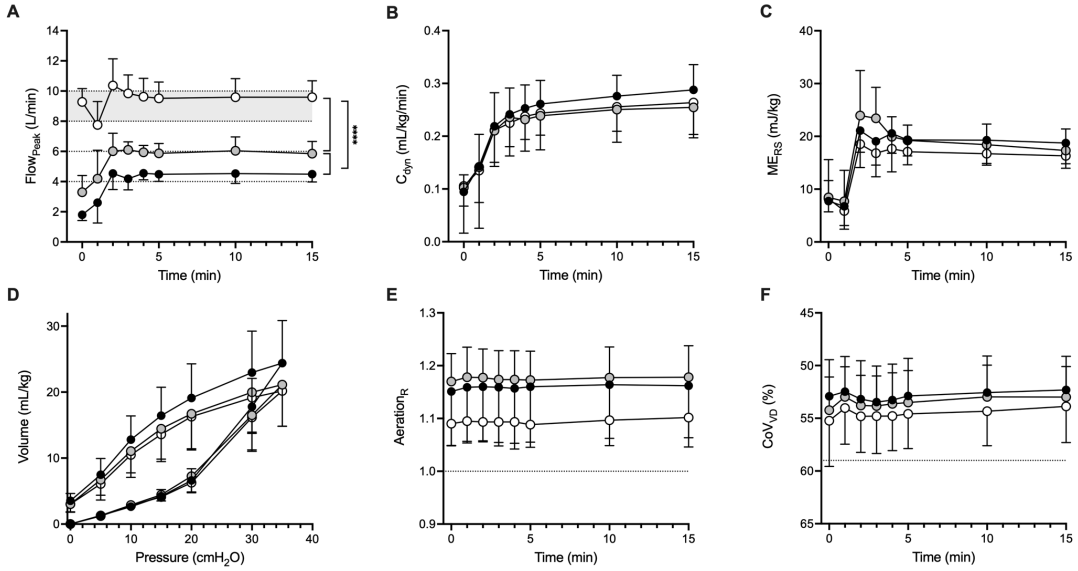

Figure 2. Peak inspiratory flow ($Flow_{Peak}$; **A**), dynamic compliance (C_{dyn}; **B**), mechanical energy of the respiratory system (ME_{RS}; **C**), static pressure-volume curve at 45 min (**D**), relative distribution of aeration in the right (**E**) lung and relative gravity dependent distribution of V_T along the right to left (CoV_{RL}; **F**) lung plane for the 15 min ventilation study groups. Relative aeration expressed as the ratio of measured aeration to ideal aeration distribution within the lung. CoV provides a single numerical value (geometric mean) of the gravity-dependent distribution of V_T within the chest. Dotted lines indicate the CoV during uniform ventilation. Values less than the value of uniform CoV indicate greater ventilation in the ventral (non-dependent) lung compared to the dorsal (dependent) lung accordingly. Black circles represent 4 L/min ($F4_{15}$), grey circles 6 L/min ($F6_{15}$) and white circles 8-10 L/min ($F8_{15}$) bias flow strategy. Data mean and SD. **** $p<0.0001$ Tukey post-test (mixed effects model).

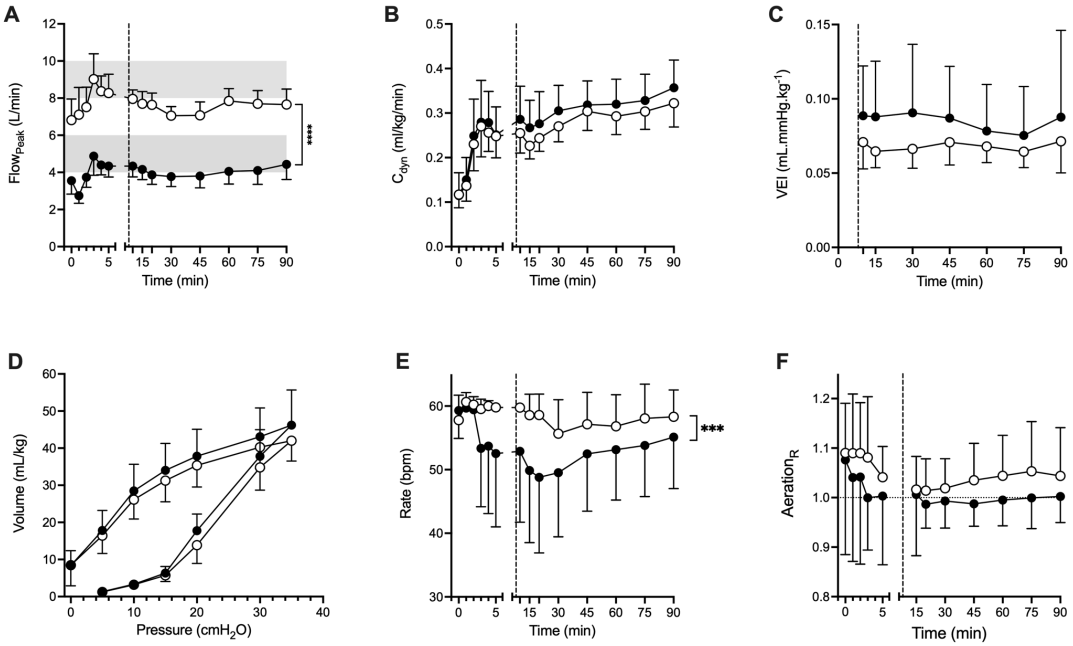

Figure 3. Peak inspiratory flow ($Flow_{Peak}$; **A**), dynamic compliance (C_{dyn}; **B**), Ventilatory Efficacy Index (VEI; **C**), static pressure-volume curve at 45 min (**D**), respiratory rate (**E**) and relative distribution of aeration in the right to left (**F**) lung plane for the 90 min ventilation study groups. Black circles represent 4 L/min ($F4_{90}$) and white circles 8-10 L/min ($F8_{90}$) bias flow strategy. Data mean and SD. Dashed vertical line represents surfactant administration. *** $p<0.001$, **** $p<0.0001$ Tukey post-test (mixed effects model).

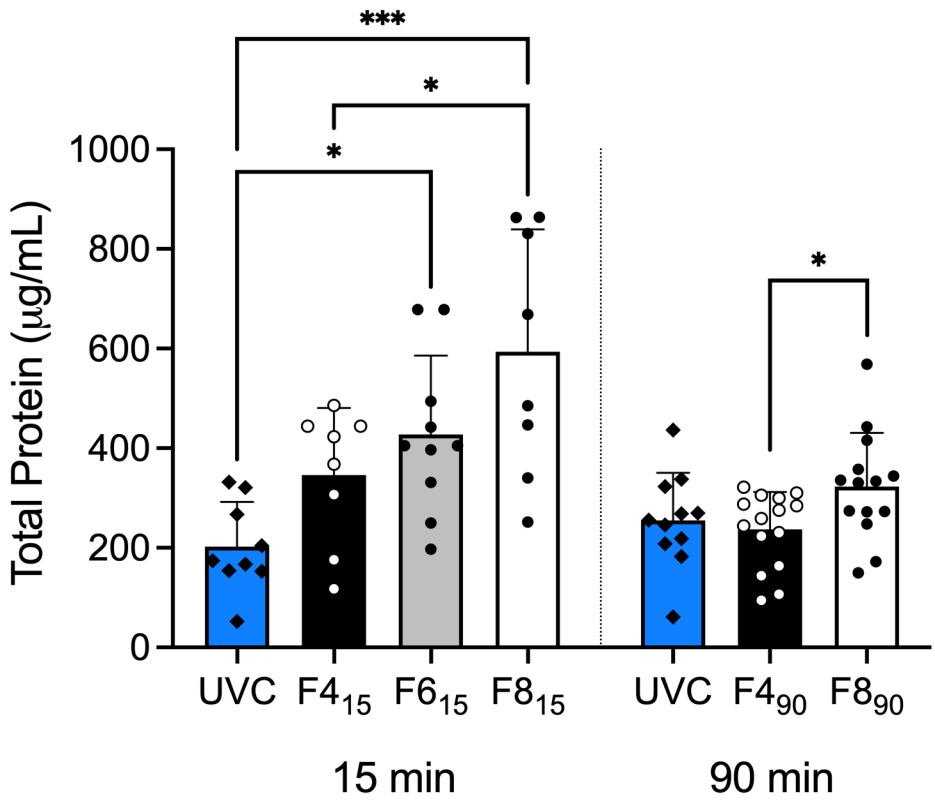

Figure 4. Total protein in the left lung lavage. Blue bars represent unventilated fetal control (UVC) lambs, black bars 4 L/min ($F4_{15}$ and $F4_{90}$) groups, grey bars 6 L/min ($F6_{15}$) and white 8-10 L/min ($F8_{15}$ and $F8_{90}$) bias flow groups for each ventilation period. Dots and diamonds represent individual lambs. All data mean and SD. * $p<0.05$, *** $p<0.001$ Tukey post-test (mixed effects model) or t-test.

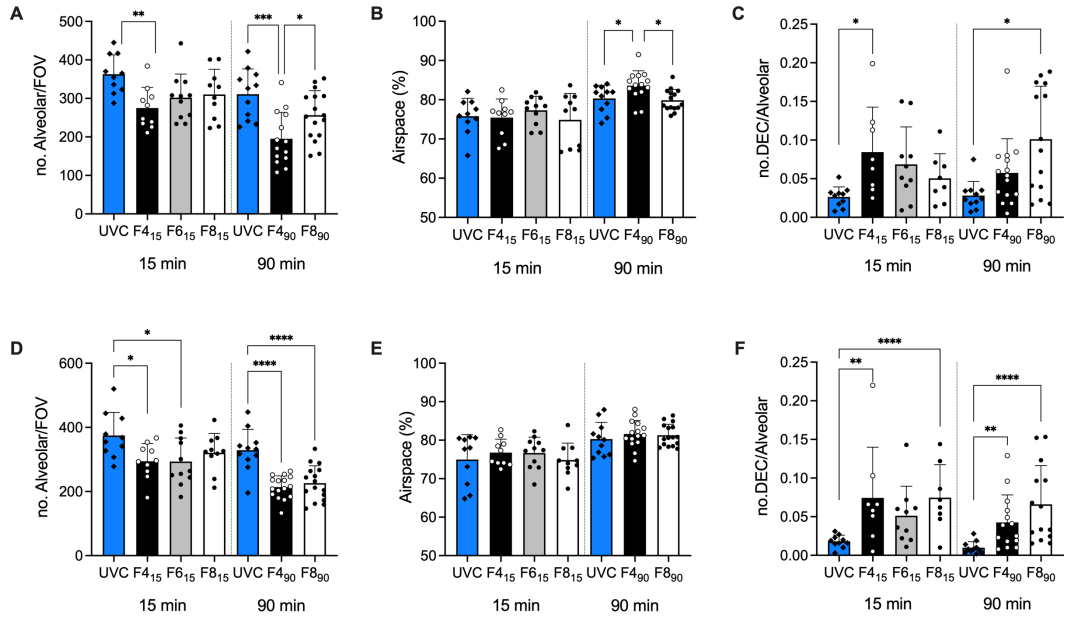

Figure 5. Number of alveoli per field of view (FOV, lower value more aerated alveoli; **A** and **D**) percentage of field of view containing airspaces (**B** and **E**) and number of detached epithelial cells per alveoli (**C** and **F**) in the gravity-non-dependent (**Panels A-C**) and gravity dependent (**Panels D-F**) right upper lobe. All 10x magnification. Blue bars represent unventilated fetal control (UVC) lambs, black bars 4 L/min ($F4_{15}$ and $F4_{90}$) groups, grey bars 6 L/min ($F6_{15}$) and white 8-10 L/min ($F8_{15}$ and $F8_{90}$) bias flow groups for each ventilation period. Dots and diamonds represent individual lambs. All data mean and SD. * $p<0.05$, ** $p<0.01$, *** $p<0.001$, **** $p<0.0001$ Tukey post-test (mixed effects model) or t-test.

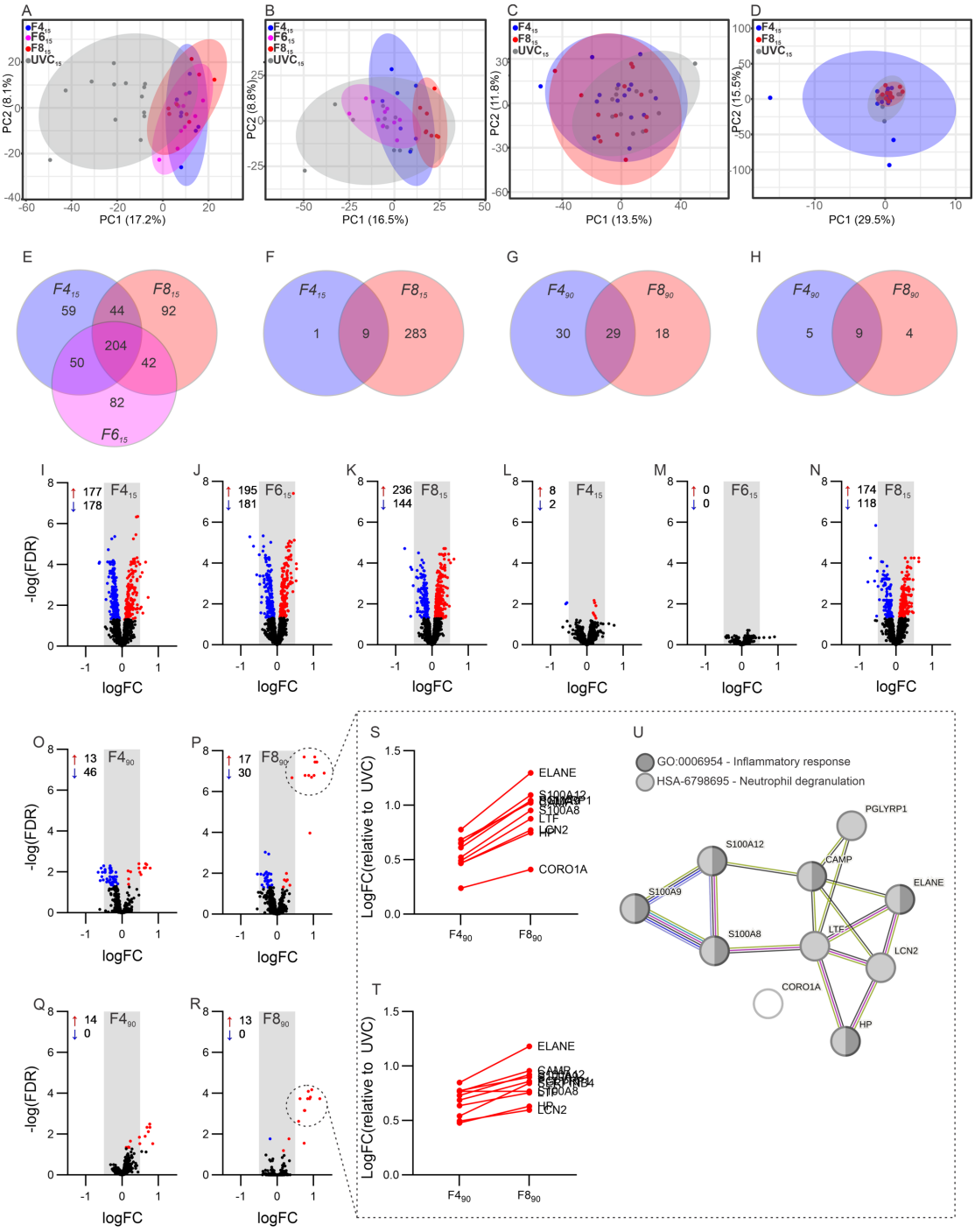

Figure 6. Proteome analysis of non-dependent and dependent lung following 15 and 90 min ventilation at different flow rates. Principal component analysis (PCA) of 15 min non-dependent (**A**), dependent (**B**), and 90 min non-dependent (**C**) and dependent (**D**) lung, with prediction ellipses depicted at a confidence interval of 0.95. Venn diagram of differentially expressed proteins (DEPs) identified in 15 min non-

dependent (**E**), dependent (**F**), and 90 min non-dependent (**G**) and dependent (**H**) lung protein datasets; QL F-test with multiplicity correction testing applied using Benjamin-Hochberg method, FDR<0.05. Volcano plots of 15 min non-dependent (**I-K**), dependent (**L-M**), and 90 min non-dependent (**O-P**) and dependent (**Q-R**) protein datasets, with DEPs that display increased abundance highlighted in red, and DEPs with decreased abundance highlighted in blue. Top 10 DEP abundance in 90 min non-dependent (**S**) and dependent (**T**) lung, represented as Log_2(Fold change) relative to UVC_{90}, and their protein-protein network interaction STRING (**U**), with high confidence (0.700) and FDR<0.0001.

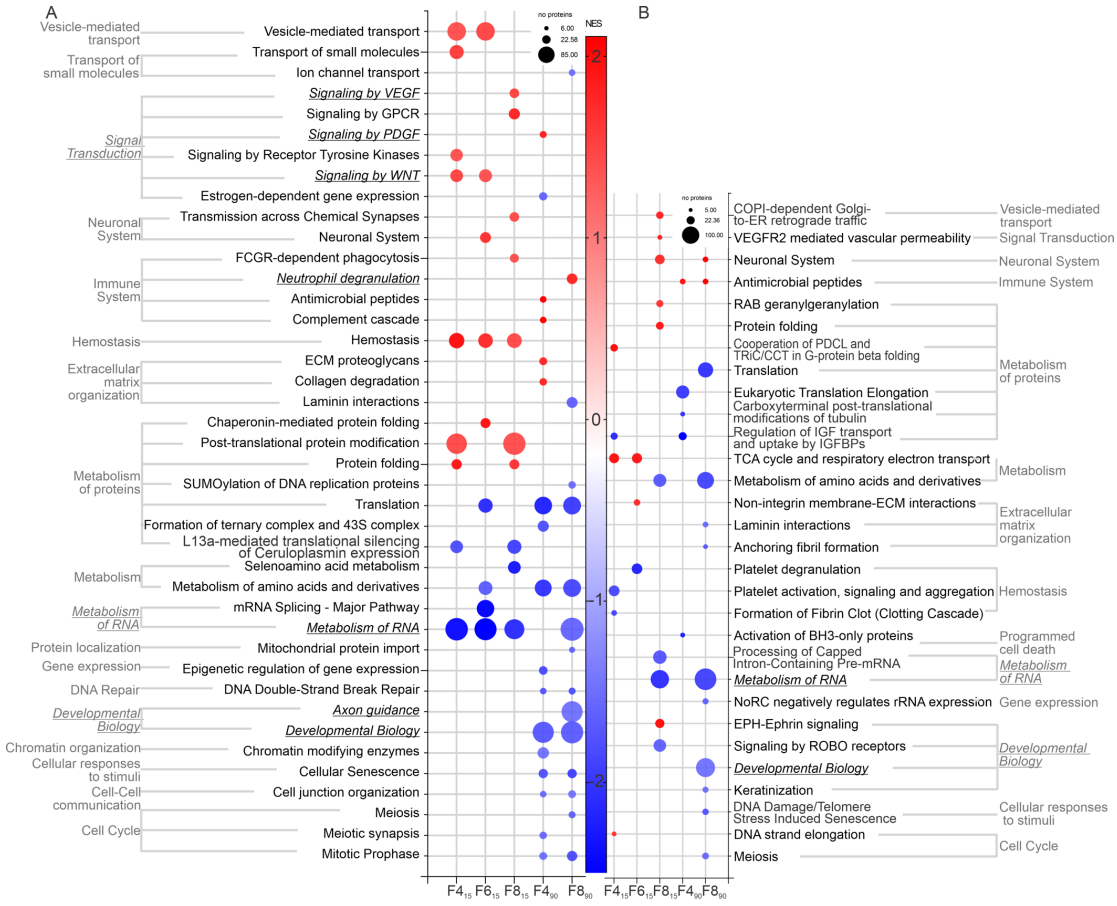

Figure 7. Gene set enrichment analysis of non-dependent and dependent lung following 15 and 90 min ventilation at different flow rates. Reactome pathways identified as enriched (NES>0; red gradient) or depleted (NES<0; blue gradient) in gene set enrichment analysis (GSEA) in non-dependent (**A**) and dependent (**B**) lung proteomes (FDR<0.05, weight-set coverage redundancy applied with pathways containing >5 proteins presented. Analysis performed in Webgestalt.). Pathways of interest are italicised and underlined. Size of circle indicates number of identified proteins in the pathway. *NES, normalised enrichment score.*

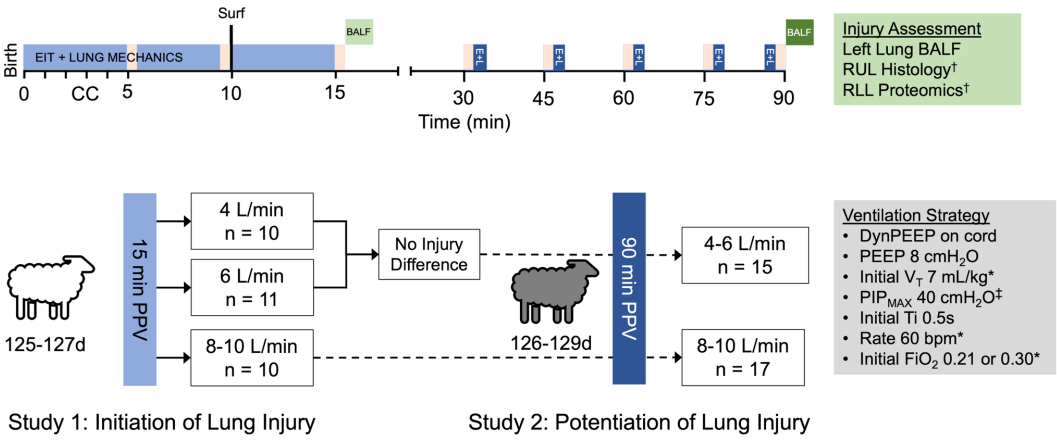

Figure 8. Summary of study design. Light blue represents methods common to both study phases. Dark blue and green represents methods limited to the 90 min positive pressure ventilation (PPV) study (**Study 2**). *Tidal volume (V_T) and PPV rate were adjusted based on arterial blood gas analysis (pink shaded boxes). Fraction of inspired oxygen (FiO_2) remained 0.21 throughout **Study 1** and was commenced at 0.30 and adjusted to maintain pre-ductal peripheral oxygen saturations 91-95% in Study 2 after the umbilical cord was cut. †Right upper (RUL) and lower (RLL) lobe histology and proteomics performed on the gravity dependent and non-dependent regions of each lobe. ‡Maximum inflation pressure (PIP_{MAX}) was set at 40 cmH_2O but transient increases to 50 cmH_2O were permitted during the initial dynamic PEEP manoeuvre (DynPEEP) at birth to facilitate aeration if needed (4, 16).

Abbreviations: CC; umbilical cord clamped, Surf; Surfactant administration (Study 2 only), E; EIT (electrical impedance tomography), L; Lung Mechanics measurements, BALF; Bronchoalveolar lavage, RUL; Right Upper Lobe, RLL; Right Lower Lobe, DynPEEP; dynamic positive end-expiratory pressure (PEEP) manoeuvre performed during PPV over 3 min with maximum PEEP 20 cmH_2O at 180s.